Perfluoroalkyl end-functionalized polystyrene show lower glass transition temperatures. DSC and optical transmission studies

H. Merve Yurdacan [a], Xiaochen Li [b, c], Steven Nutt* [b, c], Thieo E. Hogen-Esch [a,]

[a] *Department of Chemistry and Loker Hydrocarbon Research Institute, University of Southern California, Los Angeles, CA, United States*

[b] *Department of Chemical Engineering and Material Science, University of Southern California, Los Angeles, CA, United States*

[c] *Department of Aerospace and Mechanical Engineering, University of Southern California, Los Angeles, CA, United States*

* E-mail: nutt@usc.edu

Abstract: A series of polystyrenes (10-30k) end-functionalized with perfluoroalkyl (RF = C_7F_{16}, $C_{10}F_{21}$ and $C_{13}F_{27}$) groups were synthesized by atom transfer radical polymerization (ATRP) of styrene initiated by RF functionalized initiators and studied using optical transmission, differential scanning calorimetry and thermogravimetric analysis. Large decreases (40-50%) in optical transmission of the $C_{13}F_{27}$ end functionalized PS were observed compared with the non-functionalized isobaric PS consistent with the formation of large RF domains. This association increases with RF concentration and length with the latter being especially significant. A melting endotherm attributed to semi-crystalline perfluorocarbon domains was seen only for a low MW(10k) $C_{13}F_{27}$ end functionalized sample. Interestingly, compared with the matching PS, the glass transition temperatures of the RF-PS polymers were found to decrease by as much as 15 °C and with the RF lengths having the larger effects.

Key words: Polystyrene; Perfluorocarbon groups; Differential scanning calorimetry; Optical transmission

1. INTRODUCTION

Please cite the article as: H.M. Yurdacan, X. Li, S. Nutt, T.E. Hogen-Esch, **"Perfluoroalkyl end-functionalized polystyrene show lower glass transition temperatures. DSC and optical transmission studies,"** Polymer 138 (2018) 295-301. DOI: **10.1016/j.polymer.2018.01.061**

Low molecular weight (MW) perfluorocarbons (RFs) show weak intermolecular interactions compared with hydrocarbons of comparable chain lengths as expressed in much lower cohesive energy densities (δ ≈ 12 vs 15 MPa1/2) [1]. Accordingly, RFs have both pronounced hydrophobic [[2], [3], [4], [5], [6], [7], [8], [9], [10], [11]] as well as lipophobic properties [[4], [5], [6], [7], [8], [9], [10], [11], [12], [13], [14]]. Interestingly, compared to hydrocarbons, the melting points (mp's) of perfluorocarbons with eight or more carbons increase much faster with chain length [15]. For instance, while the melting points (mp's) of octane and perfluorooctane are nearly the same, the mp's of perfluorododecane and perfluorotridecane are reported to be 81 and 107 °C higher than the corresponding hydrocarbons [15]. This suggests the occurrence of much stronger intermolecular interactions for longer RFs relative to hydrocarbons. Of course that includes high MW (105-106 D) polytetrafluoroethylenes (PTFE's) that have very high mp's (∼500–621 K). This polymer has been shown to exist in four different helical crystalline states depending on temperature and pressure [16,17].

Semi-fluorinated polymers are of more recent origin and have unique properties that differ from the corresponding hydrogen or fluorocarbon polymer analogs. They have gained attention in antifouling, super-hydrophobic and self-cleaning coatings [[18], [19], [20], [21], [22], [23], [24], [25], [26], [27], [28]]. Other applications include microelectronics due to their dielectric properties [26,29], their tendency toward self-assembly [30], hydrophobic and lipophobic properties and low surface free energies [[31], [32], [33], [34]] some of which are of potential interest as organic semiconductors [28,29] and photoresponsive materials [28,35,36].

In agreement with the above, polymers containing RF or partially fluorinated pendent or end groups have been shown to exhibit mesogenic properties [[37], [38], [39], [40], [41], [42], [43], [44], [45], [46], [47], [48], [49], [50], [51], [52], [53], [54], [55]]. The effects of fluorophilic association of pendent RF groups on the rheological properties of aqueous polymer solutions [[9], [10], [11]], hydrogels [56,57] and non-aqueous polymer solutions [11] have been demonstrated.

The formation of homogeneous (1/1 w/w) blends of RF (C_7F_{15}, $C_{10}F_{21}$, $C_{13}F_{27}$) end-functionalized polystyrene (PS) and polybutylmethacrylates (PBMA) with molecular weights (MWs) in the order of 7–30k has been demonstrated recently indicating a powerful compatibilization effect especially of the longer RF end groups (C_8F_{17} or longer) [[58], [59], [60], [61]]. The degree of compatibilization i.e. the sizes of the PS and PBMA domains determined by TEM, DSC and other methods was postulated to correlate with the degree of RF end group association and strongly decreased with increasing RF size with RF end-placement being especially effective [[58], [59], [60], [61]]. For instance TEM, AFM, DSC and other methods indicated that the perfluorotridecyl (PFTD) was particularly effective in mediating RF-PS/RF-PBMA compatibilities. Thus, at a MW of ∼15k, TEM showed that the domains sizes of the PFTD end-functionalized PS and the corresponding PBMA are much smaller (∼1–3 nm) compared to that seen for the shorter RF end groups (≥10 nm) [59]. Furthermore, as indicated above, the compatibilization effects of RF end groups was far greater than the corresponding pendent groups at the same RF mass fraction and polymer MW [60,61].

The potential of perfluorocarbon (RF) end groups to influence the bulk properties of single polymers should be of interest given the above. For instance we have found that for $C_{13}F_{27}$ end-functionalized 15k PS the storage moduli between 10 and 100 Hz were increased nearly two-fold while the loss moduli increased more than four fold [62,63]. Given the small content of RF of these end-functionalized PS these surprisingly robust effects (SI Table 1) indicate the formation of the RF domains the nature and size of which, thus far, is unknown.

Here we report the optical transmission (OT), differential scanning calorimetry (DSC) and thermal gravimetric analysis (TGA) of C_7F_{15}, $C_{10}F_{23}$ and $C_{13}F_{27}$ end-functionalized polystyrenes (PS) with MW's between 10 and 30k that show evidence for formation of RF aggregates that are dependent on both RF concentration and –lengths especially for the longest PFTD end functionalized PS. Similar but much less pronounced aggregation is seen for the shorter $C_{10}F_{21}$ and C_7F_{15} end groups having approximately the same RF weight fractions with the C_7F_{15} groups giving the smallest domains.

Interestingly, DSC data of the PFTD end-functionalized PS indicate sizable decreases in Tg (as high as 15 °C) compared to the isobaric PS with similar but smaller decreases seen of the smaller RF end groups. This surprising and unprecedented finding hints at a high PS mobility mediated by the PS chain end segments being connected to RF aggregates.

2. METHODS AND MEASUREMENTS

Synthesis. The RF end functionalized polystyrenes were synthesized by atom transfer radical polymerization (ATRP) using RF-functionalized initiators synthesized via esterification of 1,1-dihydroperfluoroalcohols ($C_nF_{2n+1}CH_2OH$) with 2-bromoisobutyryl bromide (Scheme 1) [[59], [60], [61], [62], [63]]. A mixture of 20% v/v hexafluorobenzene/toluene (20/80 v/v) was used in some cases to dissolve the longer perfluoroalcohols [63]. Polymerizations were done in the presence of CuBr/N,N,N″-pentamethyldiethylene-triamine (PMDTA) and [Initiator]:[CuBr]:[Ligand] ratios of 1:1:2 at 90 °C [[59], [60], [61]]. Polydispersities (PDIs) were kept low using limited monomer conversions (~40%). The polymer solutions were passed through a silica column to remove CuBr. After concentrating the solutions the polymers were precipitated as white solids in methanol and dried at 60 °C under vacuum for 1 day. The samples are designated as PS followed by RF carbon numbers preceded by "C" followed by PS MW in kilo Daltons (Table 1). Hence PSC7-10K indicates a PS MW of around 10k having a C_7F_{15} end group.

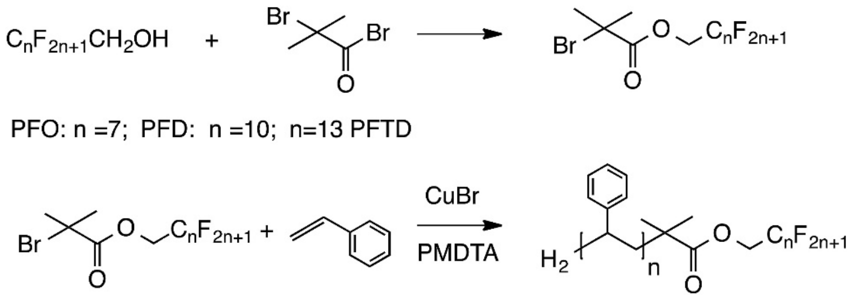

Scheme 1. Synthesis of perfluorooctyl (PFO), perfluorodecyl (PFD) and perfluorotridecyl (PFTD) initiator from their 1,1-dihydroperfluoroalcohols and their use in the ATRP polymerization of PFO, PFD and PFTD end funtionalized polystyrenes.

Table 1. Synthesis, characterization and optical transmission of PS-RF.

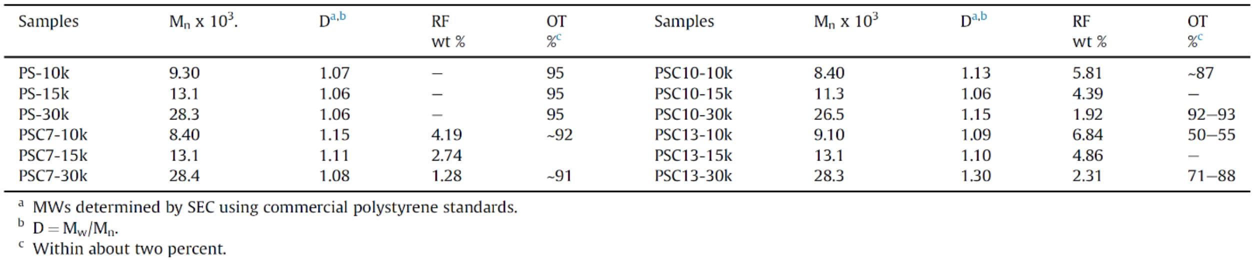

Samples	M_n x 10^3.	D[a,b]	RF wt %	OT %[c]	Samples	M_n x 10^3	D[a,b]	RF wt %	OT %[c]
PS-10k	9.30	1.07	–	95	PSC10-10k	8.40	1.13	5.81	~87
PS-15k	13.1	1.06	–	95	PSC10-15k	11.3	1.06	4.39	–
PS-30k	28.3	1.06	–	95	PSC10-30k	26.5	1.15	1.92	92–93
PSC7-10k	8.40	1.15	4.19	~92	PSC13-10k	9.10	1.09	6.84	50–55
PSC7-15k	13.1	1.11	2.74		PSC13-15k	13.1	1.10	4.86	–
PSC7-30k	28.4	1.08	1.28	~91	PSC13-30k	28.3	1.30	2.31	71–88

[a] MWs determined by SEC using commercial polystyrene standards.
[b] $D = M_w/M_n$.
[c] Within about two percent.

OT measurements. Samples for optical transmission studies were prepared by drop casting of 60 mg/ml of filtered (<0.5 mµ) toluene solutions on a micro cover glass followed by drying in a dust free conditions annealing at 120° C for 24 h followed by slow cooling over about 12 h. The thickness of the resulting films was about 5 µm.

Differential calorimetry. DSC measurements were conducted with a Differential Scanning Calorimeter (TA Instruments Q2000). Samples for thermal studies were about 10 mg in a sealed

Please cite the article as: H.M. Yurdacan, X. Li, S. Nutt, T.E. Hogen-Esch, **"Perfluoroalkyl end-functionalized polystyrene show lower glass transition temperatures. DSC and optical transmission studies,"** Polymer 138 (2018) 295-301. DOI: **10.1016/j.polymer.2018.01.061**

alumina pan and were measured under N2 flow. The sample was heated to 120 °C at a rate of 10 °C/min then cooled to 30 °C following by reheating to 180 °C. at a rate of 5 °C/min. Measurements were collected for the second run.

Thermogravimetric analyses were performed on a Shimadzu TGA-50 instrument with samples being ground into fine powders. The polymers were heated to 120 °C and were held isothermally at 120 °C for 30 min before gathering data. The TGA thermograms were measured between 25 °C and 600 °C in air at a heating rate of 5 °C/min.

3. RESULTS

Synthesis. As discussed above, a number of RF- end-functionalized PS samples were synthesized using ATRP methods used previously [59,60]. The polydispersities (PDIs) were kept low by using high monomer concentrations and limited (~40%) monomer conversions. The samples are labeled giving both RF end group carbon numbers preceded by “C” followed by the PS MW in kilo Daltons (Table 1). Hence, PSC7-10K indicates a PS MW of around 10k having a C_7F_{15} end group connected to the PS chain through a single methylene group (Scheme 1).

Optical Transmission (OT) measurements. Given the low refractive indices differences (RIs) of low MW perfluorocarbons [15] ($n \approx 1.30$) relative to polystyrene ($n = 1.59$) [1] this indicates the potential to use optical transmission for a qualitative evaluation of the size of RF-rich domains relative to optical wave lengths [60]. The optical transmissions (OTs) of the RF-PS samples and the matching PS homopolymers were carried out and are summarized in Table 1 and Fig. 1, Fig. 2, Fig. 3. The OT measurements provide merely qualitative evidence that may reflect multiple refraction associated with the formation of RF-rich micelles or similar structures [59,64]. The data in Fig. 1 show the effects of both changes in OT with wave length of PSC7-10k, PSC10-10k, PSC13-10k and

Please cite the article as: H.M. Yurdacan, X. Li, S. Nutt, T.E. Hogen-Esch, **“Perfluoroalkyl end-functionalized polystyrene show lower glass transition temperatures. DSC and optical transmission studies,”** Polymer 138 (2018) 295-301. DOI: **10.1016/j.polymer.2018.01.061**

the matching PS-10k homopolymer. Several observations are of interest. First, as shown in Fig. 1, Fig. 2, PS-10k and PS-30k are identical and nearly optically clear (OTs ~96 ± 2%) over the 350–800 nm mostly by slight Rayleigh scattering due to density fluctuations and other factors (see below) [64,65].

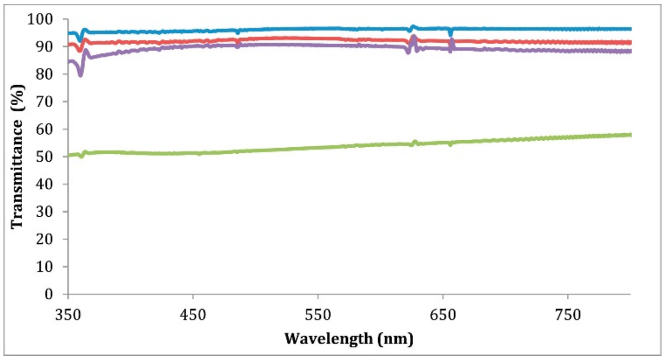

Fig. 1. UV–Visible optical transmittance versus wavelength of the PS-10k (blue), PSC7-10k (red), PSC10-10k (purple) and PSC13-10k (green) polymer films. Spectral "wiggles" at about 350, 480, 625 and 650 nm are instrument related. (For interpretation of the references to colour in this figure legend, the reader is referred to the Web version of this article.)

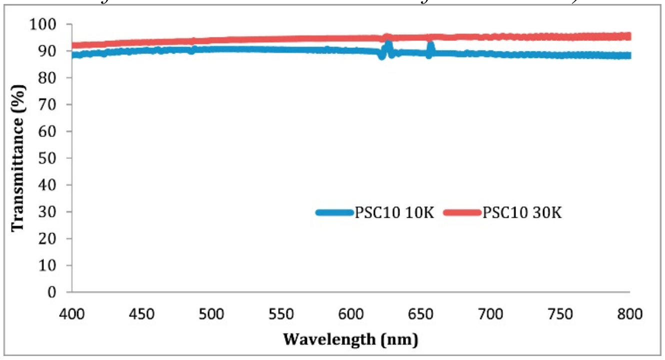

Fig. 2. UV–Visible Transmittance versus wavelength of PSC10-10K and PSC10-30K polymer films on micro cover glass. Spectral "wiggles" at about, 625 and 650 nm are instrument related.

Please cite the article as: H.M. Yurdacan, X. Li, S. Nutt, T.E. Hogen-Esch, **"Perfluoroalkyl end-functionalized polystyrene show lower glass transition temperatures. DSC and optical transmission studies,"** Polymer 138 (2018) 295-301. DOI: **10.1016/j.polymer.2018.01.061**

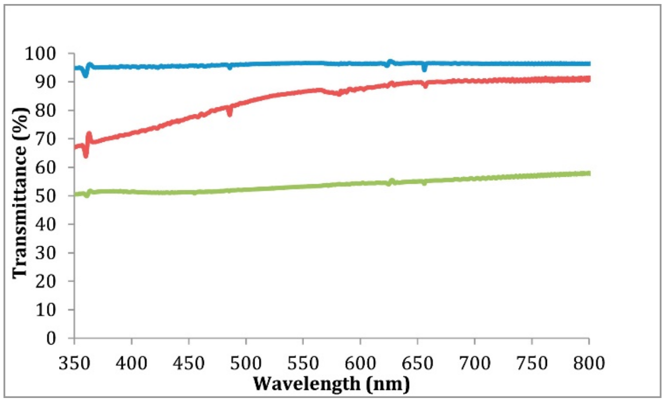

Fig. 3. UV–Visible Transmittance versus wavelength of PSC13-10K (green), PSC13-30K (red) and PS-30K (blue). Spectral "wiggles" at about 350, 480, 625 and 650 nm are instrument related. (For interpretation of the references to colour in this figure legend, the reader is referred to the Web version of this article.)

Second, small, OT decreases are seen for PSC7-10k, and PSC10-10k (OTs of 93% and 88% respectively) compared to the matching PS 10k homopolymer that are nearly wave length independent from 400 to 800 nm plausibly due to multiple refraction due to micellar aggregation of the PS-RF end groups (below) [59].

The somewhat stronger aggregation of the $C_{10}F_{21}$ end groups is also suggested for the OT data of PSC10-10k and PSC10-30K (Fig. 2) (92–95% respectively) consistent with a RF concentration driven aggregation given the concentration difference between PSC10-30k (2.0 wt % RF) and PSC10-10k sample (6.2 wt % RF) (Table 3).

In contrast, the PSC13-10k films have a white reflective appearance and show much lower OTs in the order of 0.50–0.58 (Fig. 1). This appears to indicate the presence of much larger RF rich aggregates involving domains that are large on the optical wave length scale [58,59] This is consistent with multiple refractive scattering due to the low refractive indices of perfluorocarbons and hence perfluoroalkyl groups associated into domains/micelles [15]. This effect is much more pronounced for PSC13-10k than the PSC13-30k samples the latter showing wavelength dependence with a clear increase in OT (70 to nearly 90%) as wave lengths increase from 400 to 700 nm, consistent with the presence of nm sized domains formed by an RF concentration driven association [59,62]. (Fig. 3). In contrast the OTs of the PSC13-10k is opaque at all wave lengths with an OT values of about 50–55%.

Given the above, the effect of the $C_{13}F_{27}$ end groups is especially dominant. For instance, in PSC13-30k the calculated RF content (2.4 wt %) is lower than that of PSC7-10k (4.4 wt %) or PSC10-10k (6.2 wt%) both of which show much higher OT values below 650 nm. This appears to be consistent with an especially strong aggregation of the large $C_{13}F_{27}$ end groups that was also seen for the compatibilization of RF- end functionalized PS and polybutylmethacrylates (PBMA) [[55], [56], [57], [58], [59], [60], [61], [62]]. In this case the compatibilization effects of the $C_{13}F_{27}$ end groups were far greater than seen for the $C_{10}F_{21}$ and C_7F_{15} end groups.

Data consistent with the present RF-PS polymers were seen by nano-indentation measurements of very similar RF-PS polymers showing dramatic increases in storage (E') and especially loss (E'') moduli for PS13-15k ($E'' = 1.46$ GPa) compared to PSC13-30k ($E'' = 0.38$ GPa) [62]. In spite of these strong correlations the nature of the RF micellar structures is unclear (see below). Given the above, both RF length and -concentration are important but the effects are especially strong ($\Delta Tg=11$ °C) for the largest RF groups even at the highest PS MW (Table 2). Furthermore, given the qualitative nature of the OT data the shape size of the RF micelles are uncertain and would require more detailed studies (see Discussion).

Table 2. Glass transition temperatures of RF End Functionalized Polystyrenes and the corresponding PS homopolymers.

Please cite the article as: H.M. Yurdacan, X. Li, S. Nutt, T.E. Hogen-Esch, **“Perfluoroalkyl end-functionalized polystyrene show lower glass transition temperatures. DSC and optical transmission studies,”** Polymer 138 (2018) 295-301. DOI: **10.1016/j.polymer.2018.01.061**

Samples	RF^{a} (wt%)	T$_{g}$^{b} (^{0}C)	ΔT$_{g}$^{c} (^{0}C)	Samples	RF^{a} (wt%)	T$_{g}$^{b} (^{0}C)	ΔT$_{g}$^{c} (0C)
PS-10k	–	91.3	–	PSC10-15k	4.1	93.8	4.2
PSC7-10k	4.4	87.4	3.9	PSC13-15k	5.1	90.0	9.0
PSC10-10k	6.2	84.3	7.0	PS-30k	–	102	–
PSC13-10k[d]	7.4	76.2	15.1	PSC7-30k	1.3	99.0	3.0
PS-15k		99.0		PSC10-30k	2.0	98.3	3.7
PSC7-15k	2.8	98.0	1.0	PSC13-30k	2.4	90.6	11.4

[a] Calculated values based on Mn.

[b] Average of the "onset" and "end" of the glass transition process as indicated as deviation and resumption from linearity.

[c] Decreases in Tg.

[d] Melting point is seen at 130–135° C (Fig. 4).

Differential Scanning Calorimetry. The thermal properties of perfluorocarbon (RF) end-functionalized polymers in the context of the above OT and other data on these new RF-PS type polymers could be interesting for several reasons. First, the effect of RF length and content on the glass transitions (Tg's) of the RF-end functionalized PS in the bulk is expected to be significant in that chain end RF groups are known to associate to varying degrees in virtually all media other than fluorocarbon solvents consistent with the above OT and other studies [[3], [4], [5], [6], [7],11,42,43]. Similarly, the OT data especially of PSC13-10k have indicated the presence of very large RF domains exceeding visible wave lengths.

Such associations should affect the segmental motions of the PS chain segments adjacent to the RF end groups. This may be expected to affect glass transition temperatures (Tgs) especially for the smaller polymers (PSC13-10k) where the RF concentrations are highest and end group effects should be pronounced. Hence the differential scanning calorimetry is of special interest. As shown in Fig. 4 and Table 2, the presence of all RF end groups, surprisingly, give decreases in Tg values. Moreover the magnitude of the decreases increases with RF length for each MW (Table 2). For

Please cite the article as: H.M. Yurdacan, X. Li, S. Nutt, T.E. Hogen-Esch, **"Perfluoroalkyl end-functionalized polystyrene show lower glass transition temperatures. DSC and optical transmission studies,"** Polymer 138 (2018) 295-301. DOI: **10.1016/j.polymer.2018.01.061**

instance PSC7-10k, PSC10-10k and PSC13-10k show ΔTg values of 3.9, 7.0 and 15.1 °C respectively (Table 2). This is also for PSC13-15k, and PSC13-30k as illustrated in Fig. 4.

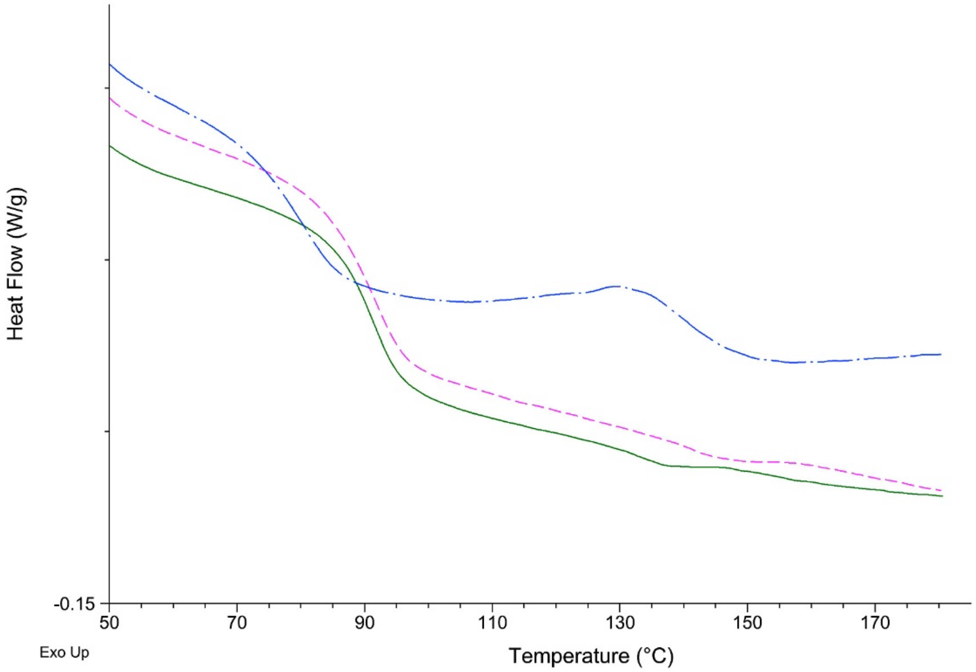

Fig. 4. DSC thermograms of PSC13 polymers with varying molecular weights. PSC13-10k (Blue), PSC13-15k (Green), PSC13-30k (Pink). Measurements were taken at second runs and the samples were heated under nitrogen to 180 °C at a rate of 5 °C/min. (For interpretation of the references to colour in this figure legend, the reader is referred to the Web version of this article.)

Decreases in Tg with increased RF content are also seen. For instance the Tg values for PSC10-10k, PSC10-15k and PSC10-30k having the same C10F21 end group with RF concentrations of 6.2, 4.1 and 2.0 wt % give ΔTg values of 7.0, 4.2 and 3.7 °C respectively (Table 2). The effects tend to be greater for longer RF end groups at the same RF weight fractions. Overall the RF end group effects are qualitatively similar to changes in OT but in this case the smaller RF groups appear to still show relatively significant effects.

Of special additional interest is the presence of a clear endotherm for PSC13-10k at 130–135 °C as shown in Fig. 4. The clear endotherm may be consistent with the presence of crystalline or semi-crystalline domains [[37], [38], [39], [40], [41], [42], [43], [44], [45], [46], [47], [48], [49],

[50], [51], [52], [53], [54], [55]]. Such domains may be expected given the relatively high melting point of C13F28 (100 °C) [15]. Hints of perhaps similar features are seen for PSC13-15k, PSC13-30k and PSC10-10k but none are pronounced.

Thermogravimetric analysis. The thermal degradation of PS has been studied extensively [[65], [66], [67], [68]]. It has been shown that end chain functionalization can have a substantial effect on the thermal polymer stability. Like the polymerization, the radical mediated thermal degradation of polystyrene involves initiation, propagation, chain transfer and termination steps that involve (a) random (b) chain chain-end scission, (c) back-biting, and (d) disproportionation [68]. A somewhat similar mechanism for RF-end-functionalized PS may occur except that the presence of the RF chain end could affect the decomposition. Accordingly TGA measurements were carried out on the shortest (C_7F_{15}) and longest ($C_{13}F_{27}$) end-functionalized PS. The thermal degradation of PS-10K (Fig. 5) starts at about 280 °C but the PSC7-10K and PSC10-10K showed slower degradation consistent with end group initiated decomposition. This does not seem surprising given the low MW's. This behavior is also seen for samples PS-15k, PSC7-15k and PSC13-15k with the later two showing almost identical behavior (Fig. SI 2).

Please cite the article as: H.M. Yurdacan, X. Li, S. Nutt, T.E. Hogen-Esch, **“Perfluoroalkyl end-functionalized polystyrene show lower glass transition temperatures. DSC and optical transmission studies,”** Polymer 138 (2018) 295-301. DOI: **10.1016/j.polymer.2018.01.061**

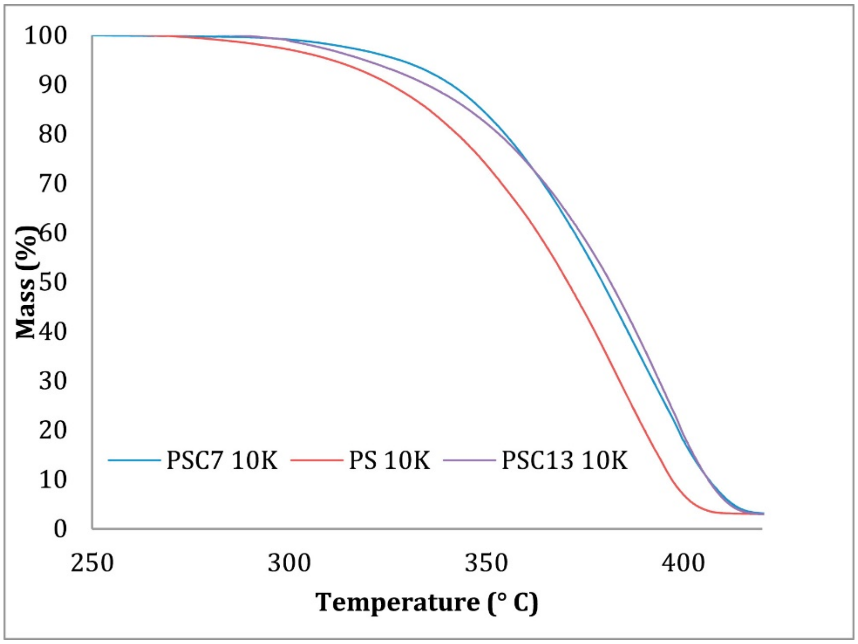

Fig. 5. TGA curves of PS 10K (red), PSC7 10K (blue) and PSC13 10K (purple). (For interpretation of the references to colour in this figure legend, the reader is referred to the Web version of this article.)

In contrast to the DSC and OT data, the effects of RF lengths were found to be almost negligible for PSC7 10K and PSC13 10K (Fig. 5). The results for samples PSC7-15K and PSC10-15K are even closer (Fig. SI 2) confirming that RF size does not play a significant role in the decomposition.

4. DISCUSSION

OT effects. The above has shown two major effects of the RF length and concentration on association on the OT, and DSC data. The first is the much stronger OT effects of the PSC13 polymers plausibly through multiple light refraction mediated by large RF-rich domains suspended in the PS matrix. A similar RF length effect was also seen case for the analogous RF-P/RF-PBMA blends where the blending effectiveness of the $C_{13}F_{27}$ end groups was found to be much greater than the smaller RF groups [[58], [59], [60]]. Given the large differences in cohesive energy densities and refractive indices of 1.59 and ~1.3 of PS and fluorocarbons respectively, the occurrence of multiple refractive scattering of visible light is not surprising. Thus at the lowest polymer MW (PSC13-10K) and hence highest $C_{13}F_{27}$ concentrations the RF or RF- rich domains are plausibly large compared with the optical wave lengths resulting in multiple refractive scattering and hence little wavelength dependence (Fig. 3). At lower RF group concentrations (PSC13-30k), the RF domains appear to be smaller on the 400–800 nm length scale consistent with its stronger OT wavelength dependence (Fig. 3). This strong dependence of $C_{13}F_{27}$ concentration on domain size is consistent with aggregation of a large number for RF groups to associate into micellar structures (Scheme 2). These scheme shows associated RF groups with attached PS chains being subject to excluded volume restrictions. Although the details of these structures are unclear, elongated micelles are expected.

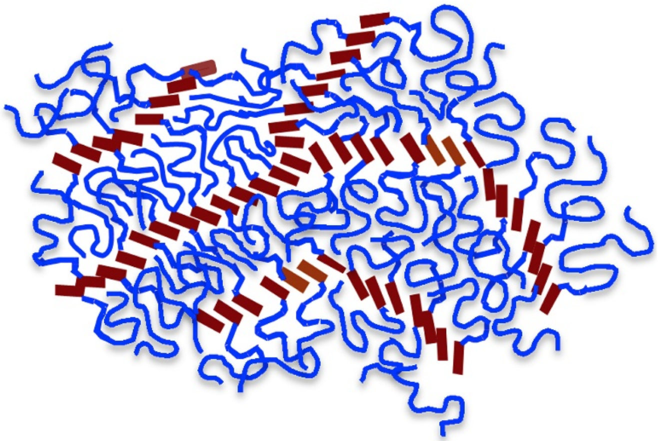

Scheme 2. Proposed association of PFTD end-functionalized PS (Low MW 10K-15K) in bulk.

Given the high density of the RF groups (1.7–1.9 g/mL, Ref.15), volume fractions of the RF groups only amount about to 0.8–3.6% thus making the ordering in well defined supra-molecular structures less likely. Furthermore, with the exception of one polymer (PSC13-10-k) the DSC analysis, with one exception (PSC13-10k) did not show the presence of endotherms associated with crystalline domains. Even in that case the endotherm was small and broad (Fig. 4). As the RF domains are separated by what appear to be large (10-30k) amorphous PS domains the use of wide angle X ray scattering is not likely to produce useful results.

The association of the RF groups depends in turn on (a) the cohesive energy densities differences between RF-rich and PS-domains and (b) their refractive index differences [1,4,6,15,[59], [60], [61], [62]]. The enthalpy (ΔHm) of mixing polystyrene with RF groups may be estimated to a first approximation by the heat of mixing (ΔHm) of the simple PS-RF binary mixtures. This would lead to [1].

$\Delta H_m = V.(\Delta_1 - \Delta_2)^2\ \varphi_1.\varphi_2$ (1) $\Delta i = (\Delta E^V{}_i/V_i)^{1/2}$ (2)

where V and φ_i are the total volume and volume fractions of the PS and the RF component and Δ_1 and Δ_2 are the cohesive energy densities and $\Delta E^V{}_i$ are the corresponding energy changes on isothermal vaporization.

Hence the formation of the RF and PS phases would be expected to be enthalpy favored although from eqn-1 the ΔH_m would be expect to be small based on the values of Δ_1 and Δ_2 (18 ± 0.5 MPa$^{1/2}$ and ($\Delta_2 = 12 \pm 0.7$ MPa$^{1/2}$) respectively and the low volume fractions (0.8–3.6%) of the RF groups. It is clear that this does not account for the unusually strong effects of RF length. However the entropies of RF domain formation should be favored for the longer RF groups. For instance, given micelle formation and at given values of φ_2, the number partially immobilized number of PS chains as a result of RF domain formation would be smaller for longer RF chains.

DSC effects. Second, sizable decreases of Tg were seen for all RF end groups especially for the longest and highest concentrations of RF end groups. To the best of our knowledge such effects have not been observed thus far. As noted above the decreases in Tg are especially large for the PSC13 polymers with smaller effects being seen at higher RF concentrations (Table 2). The decreases in Tg suggest rapid motions of the RF chains that increase with RF length that my be conceivably entropy driven (positive ΔS). The extraordinary conformational mobility of perfluorocarbons in the form of rapid helix (ps time scale) reversals has been noted for some crystalline forms of polytetrafluoroethylene (PTFE) at ambient temperatures [16]. For the much lower MWs of the RF end groups the corresponding smaller topological restraints for the present PS-RF polymers should allow similar helix reversal based motions that may increase the mobility of the of the adjacent PS chain segments even at higher PS MWs. This would be especially true for the longer RF groups for which such helical structures should be more accessible. This is consistent with what we see for the unusual decreases in Tg with increased RF content and, especially, length. These unusual RF effects on PS segmental mobility are consistent with nano-indentation studies (see below).

Nano-indentation *measurements*. These have shown that, compared to the isobaric PS, the elastic- and loss moduli of the PSC13-15k were increased about 2 and 4- fold respectively (Table 3) [62]. Smaller but still significant increases in E' (40%) and E'' (56%) were seen for PSC10-10K compared with the isobaric and un-functionalized polymer (Table 3). Such increases in both E′ and E″ appear to be related to the formation of organized structures in the form of perhaps semicrystalline domains. However this behavior does not preclude the occurrence of very rapid motions of the longer RF chains [16].

Table 3. Mechanical properties RF end-functionalized PS obtained by nano-indentation. [a]

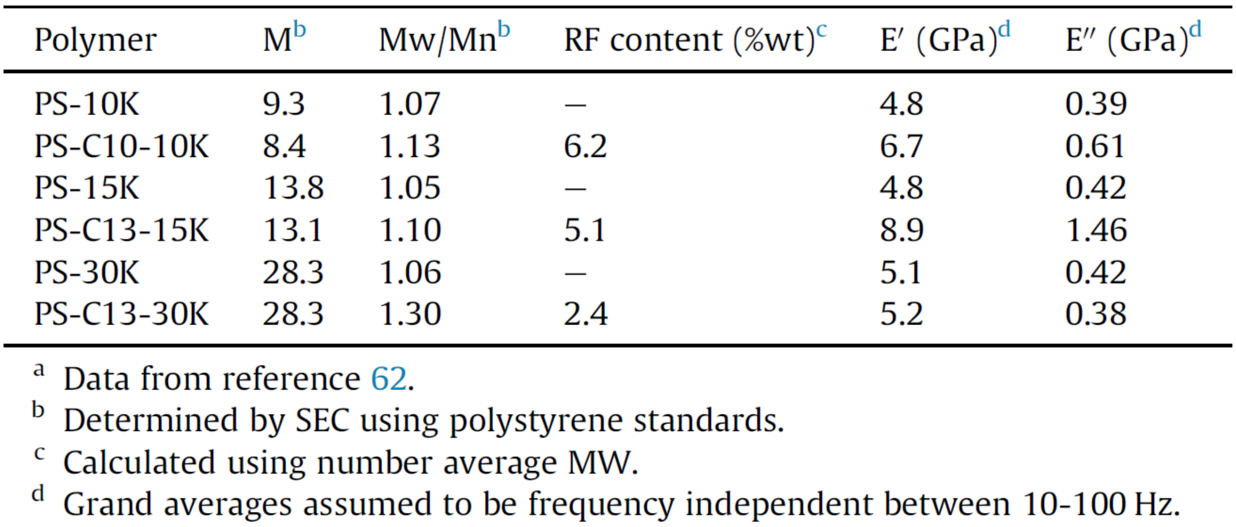

Polymer	M[b]	Mw/Mn[b]	RF content (%wt)[c]	E′ (GPa)[d]	E″ (GPa)[d]
PS-10K	9.3	1.07	–	4.8	0.39
PS-C10-10K	8.4	1.13	6.2	6.7	0.61
PS-15K	13.8	1.05	–	4.8	0.42
PS-C13-15K	13.1	1.10	5.1	8.9	1.46
PS-30K	28.3	1.06	–	5.1	0.42
PS-C13-30K	28.3	1.30	2.4	5.2	0.38

[a] Data from reference 62.
[b] Determined by SEC using polystyrene standards.
[c] Calculated using number average MW.
[d] Grand averages assumed to be frequency independent between 10-100 Hz.

The increases noted for in both moduli for PSC13-10k and for PSC13-15k are interesting given the decreases in Tg seen for these polymers (Table 2) with much smaller effects being seen for the C_7F_{15} end groups. As inferred from the DSC data this may consistent with what the association of the perfluorotridecyl groups into what appear to be semicrystalline micellar domains at least for the case of PSC13-10k. Interestingly the moduli for PSC13-30k were not changed indicating that the presence of RF-micelles does not appear to correlate with mechanical properties at ambient temperatures for the higher MW PS-RF polymers. However rheological studies determined on PSC13-30k do show significant RF effects at higher temperatures [63]. This hints at the importance of the motions of the RF and PS chain segments occurring at very different time scales.

5. CONCLUSIONS

The optical transmission and differential scanning calorimetry of C_7F_{15}, $C_{10}F_{21}$ and $C_{13}F_{27}$ end functionalized polystyrenes indicates a fluorophilic association into what appear to be RF micellar domains. This association is far more pronounced for the longest end groups with much

Please cite the article as: H.M. Yurdacan, X. Li, S. Nutt, T.E. Hogen-Esch, **“Perfluoroalkyl end-functionalized polystyrene show lower glass transition temperatures. DSC and optical transmission studies,”** Polymer 138 (2018) 295-301. DOI: **10.1016/j.polymer.2018.01.061**

weaker effects seen for the smaller C_7F_{15} and $C_{10}F_{21}$ groups. All groups show decreases in Tg of the PS with RF lengths and higher RF concentrations with length effects being more the more important with largest Tg decreases (up to 15 °C) seen for the $C_{13}F_{27}$ groups in PSC13-10k. For the polymer only, the presence of a small endotherm around 130 °C suggests the presence of RF (semi)-crystalline domains. The associative properties of the RF groups are enthalpy and plausibly entropy driven. The data are fully consistent in part with earlier nano-indentation results on these polymers.

Acknowledgements: This research was supported by the Loker Hydrocarbon Research Institute that has included several stipends to one of us (MY).

References:

1. J. Brandrup, E.H. Immergut and E.A. Grulke Eds, Polymer Handbook, fourth ed., Wiley and Sons, New York, NY, (Chapter 7).
2. V.H. Dalvi, P.J. Rossky, Molecular origins of fluorocarbon hydrophobicity, Proc. Natl. Acad. Sci. Unit. States Am., 107 (31) (2010), pp. 13603-13607
3. M.P. Krafft, J.G. Riess, Chemistry, physical chemistry, and uses of molecular Fluorocarbon−hydrocarbon diblocks, triblocks, and related compounds-unique “apolar” components for self-assembled colloid and interface engineering, Chem. Rev., 109 (5) (2009), pp. 1714-1792
4. J.A. Gladysz, D.P. Curran, I.T. Horvath, Handbook of Fluorous Chemistry, John Wiley & Sons (2006)
5. J.G. Riess, Highly fluorinated amphiphilic molecules and self-assemblies with biomedical potential, Curr. Opin. Colloid Interface Sci., 14 (5) (2009), pp. 294-304
6. A. Pittman L.A. Wall (Ed.), Fluoropolymers, Wiley-Interscience, New York (1972)
7. J.M. Vincent, Noncovalent associations in fluorous fluids, J. Fluorine Chem., 129 (10) (2008), pp. 903-909
8. R.C. Liu, F.M. Winnik, Synthesis and spectroscopic characterization of fluorescently labeled hydrocarbon-and/or fluorocarbon-modified poly (sodium 2-acrylamido-2-methylpropanesulfonates), J. Photochem. Photobiol. Chem., 178 (2) (2006), pp. 208-219
9. Y.X. Zhang, A.H. Da, G. Butler, T. Hogen-Esch, A fluorine-containing hydrophobically associating polymer. I. Synthesis and solution properties of copolymers of acrylamide and fluorine-containing acrylates or methacrylates, J. Polym. Sci., Part A: Polym. Chem., 30 (7) (1992), pp. 1383-1391
10. T.A. Seery, M. Yassini, T.E. Hogen-Esch, E.J. Amis, Static and dynamic light scattering characterization of solutions of hydrophobically associating fluorocarbon-containing polymers, Macromolecules, 25 (18) (1992), pp. 4784-4791

Please cite the article as: H.M. Yurdacan, X. Li, S. Nutt, T.E. Hogen-Esch, **“Perfluoroalkyl end-functionalized polystyrene show lower glass transition temperatures. DSC and optical transmission studies,”** Polymer 138 (2018) 295-301. DOI: **10.1016/j.polymer.2018.01.061**

11. J. Da, T.E. Hogen-Esch, Poly(N,N-dimethylacrylamide)s with perfluorocarbon pendent groups connected through poly(ethylene glycol) tethers give physical gels in organic solvents, Macromolecules, 36 (25) (2003), pp. 9559-9563

12. S. Qin, W.Z. Yuan, H. Li, Y. Zhang, Order–order phase transition and transformation in co-assembled ps from fluorinated FA/FB type diblock copolymers, Soft Matter, 8 (32) (2012), pp. 8405-8412

13. P. Ballester, A. Vidal-Ferran, P.W. van Leeuwen, 2 modern strategies in supramolecular catalysis, Adv. Catal., 54 (2011), p. 63

14. T. Schuster, S. Schellenberger, R. Friedrich, M. Klapper, K. Muellen, Branched fluorinated amphiphiles based on carbohydrates, J. Fluorine Chem., 154 (2013), pp. 30-36

15. P. Lo Nostro, Phase separation properties of fluorocarbons, hydrocarbons and their copolymers, Adv. Colloid Interface Sci., 56 (1995), pp. 245-287

16. E.S. Clark, The crystal structure of polytetrafluoroethylene, forms I and IV, J. Macromol. Sci., Part B: Physics, 45 (2) (2006), pp. 201-213

17. T. Suwa, T. Seguchi, M. Takehisa, S. Machi, Effect of molecular weight on the crystalline structure of polytetrafluoroethylene as-polymerized, J. Polym. Sci. Polym. Phys. Ed, 13 (11) (1975), pp. 2183-2194

18. N. Mael, F. Guittard, S. Géribaldi, Stable superhydrophobic and lipophobic conjugated polymers films, Langmuir, 22 (7) (2006), pp. 3081-3088

19. Y. Li, Y. Su, X. Zhao, R. Zhang, J. Zhao, X. Fan, Z. Jiang, Surface fluorination of polyamide nanofiltration membrane for enhanced antifouling property, J. Membr. Sci., 455 (2014), pp. 15-23

20.
J.P. Youngblood, L. Andruzzi, C.K. Ober, A. Hexemer, E.J. Kramer, J.A. Callow, M.E. Callow, Coatings based on side-chain ether-linked poly (ethylene glycol) and fluorocarbon polymers for the control of marine biofouling, Biofouling, 19 (2003), pp. 91-98

21. S. Krishnan, A. Ramakrishnan, A. Hexemer, J.A. Finlay, K.E. Sohn, R. Perry, C.K. Ober, E.J. Kramer, M.E. Callow, J.A. Callow, D.A. Fischer, Anti-biofouling properties of comblike block copolymers with amphiphilic side chains, Langmuir, 22 (11) (2006), pp. 5075-5086

22. H.S. Sundaram, Y. Cho, M.D. Dimitriou, J.A. Finlay, G. Cone, S. Williams, D. Handlin, J. Gatto, M.E. Callow, J.A. Callow, E.J. Kramer, C.K. Ober, Fluorinated amphiphilic polymers and their blends for fouling-release applications: the benefits of a triblock copolymer surface, ACS Appl. Mater. Interfaces, 3 (9) (2011), pp. 3366-3374

23. W.-J. Yang, K.-G. Neoh, E-T, S. Kang, L.-M. Teo, D. Rittschof, Polymer brush coatings for combating marine biofouling, Prog. Polym. Sci., 39 (5) (2014), pp. 1017-1042

24. D. Thierry, E. Taffin de Givenchy, F. Guittard, Superhydrophobic surfaces of electrodeposited polypyrroles bearing fluorinated liquid crystalline segments, Macromolecules, 43 (22) (2010), pp. 9365-9370

25. D. Park, C.J. Weinman, J.A. Finlay, B.R. Fletcher, M.Y. Paik, H.S. Sundaram, M.D. Dimitriou, K.E. Sohn, M.E. Callow, J.A. Callow, D.L. Handli, C.L. Willis, D.A. Fischer, E.J. Kramer, C.K. Ober, Amphiphilic surface active triblock copolymers with mixed hydrophobic and hydrophilic side chains for tuned marine fouling-release properties, Langmuir, 26 (12) (2010), pp. 9772-9781

26. Y.-C. Su, F.-C. Chang, Synthesis and characterization of fluorinated polybenzoxazine material with low dielectric constant, Polymer, 44 (26) (2003), pp. 7989-7996

Please cite the article as: H.M. Yurdacan, X. Li, S. Nutt, T.E. Hogen-Esch, **“Perfluoroalkyl end-functionalized polystyrene show lower glass transition temperatures. DSC and optical transmission studies,”** Polymer 138 (2018) 295-301. DOI: **10.1016/j.polymer.2018.01.061**

27. L.R. Hutchings, N.M. Sarih, R.L. Thompson, Multi-end functionalized polymer additives synthesised by living anionic polymerisation-the impact of additive molecular structure upon surface properties, Polym. Chem., 2 (4) (2011), pp. 851-861

28. G.E. McCluskey, S.E. Watkins, A.B. Holmes, C.K. Ober, J.-K. Lee, W.H. Wallace Wong, Semi-perfluoroalkyl polyfluorene with varying fluorine content: synthesis and photophysical properties, Polym. Chem., 4 (20) (2013), pp. 5291-5296

29. H.-G. Jeong, B. Lim, D. Khim, M. Han, J. Lee, J. Kim, J.-M. Yun, K. Cho, J.-W. Park, D.-Y. Kim, A novel thermally reversible soluble-insoluble conjugated polymer with semi-fluorinated alkyl chains: enhanced transistor performance by fluorophobic self-organization and orthogonal hydrophobic patterning,, Adv. Mater., 25 (44) (2013), pp. 6416-6422

30. M.K. Bernett, N.L. Jarvis, W. Zisman, Surface activity of fluorinated organic compounds at organic liquid—air interfaces.,, Part Iv. Effect of structure and Homology1 J. Phys. Chem., 66 (2) (1962), pp. 328-336

31. R. Ramharack, T.H. Nguyen, Fluoropolymers of very low surface energies, J. Polym. Sci. C Polym. Lett., 25 (3) (1987), pp. 93-98

32. I.J. Park, S.-B. Lee, C.K. Choi, K.-J. Kim, Surface properties and structure of poly (perfluoroalkylethyl methacrylate), J. Colloid Interface Sci., 181 (1) (1996), pp. 284-288

33. C.J. Drummond, G. Georgaklis, D.Y.C. Chan, Fluorocarbons: surface free energies and van der Waals interaction, Langmuir, 12 (11) (1996), pp. 2617-2621

34. H.M. Scholberg, R.A. Guenthner, R.I. Coon, Surface chemistry of fluorocarbons and their derivatives, J. Phys. Chem., 57 (1953), pp. 923-925

35. M.Y. Paik, S. Krishnan, F. You, X. Li, A. Hexemer, Y. Ando, S.H. Kang, D.A. Fischer, E.J. Kramer, C.K. Ober, Surface organization, light-driven surface changes, and stability of semifluorinated azobenzene polymers, Langmuir, 23 (9) (2007), pp. 5110-5119

36. A. Sanae, S. Péralta, O. Fichet, D. Teyssié, S. Cantin, Poly (azobenzene acrylate-co-fluorinated acrylate) spin-coated films: influence of the composition on the photo-controlled wettability, Langmuir, 29 (30) (2013), pp. 9499-9509

37. L. Andruzzi, F. D'Apollo, G. Galli, B. Gallot, Synthesis and structure characterization of liquid crystalline polyacrylates with unconventional fluoroalkylphenyl mesogens, Macromolecules, 34 (22) (2001), pp. 7707-7714

38. J. Höpken, C. Pugh, W. Richtering, M. Möller, Melting, crystallization, and solution behavior of chain molecules with hydrocarbon and fluorocarbon segments, Makromol. Chem., 189 (1988), pp. 911-925

39. E. Shivakumar, K. Pandey, S. Alam, C. Das, Influence of interactions on the mechanical, morphological and thermal properties of in situ ternary composites based on fluorocarbon elastomer, acrylic elastomer and liquid crystalline polymer blends, Polym. Int., 54 (10) (2005), pp. 1458-1465

40. Y.F. Zhu, H.J. Tian, H.W. Wu, D.Z. Hao, Y. Zhou, Z. Shen, D.C. Zou, P.C. Sun, X.H. Fan, Q.F. Zhou, Ordered nanostructures at two different length scales mediated by temperature: a triphenylene-containing mesogen-jacketed liquid crystalline polymer with a long spacer, J. Polym. Sci., Part A: Polym. Chem., 52 (3) (2014), pp. 295-304

41. M. Goel, M. Jayakannan, C-H/π-Interaction-Guided self-assembly in π-conjugated oligomers, Chem. Eur J., 18 (10) (2012), pp. 2867-2874

42. J. Wang, C.K. Ober, Self-organizing materials with low surface energy: the synthesis and solid-state properties of semifluorinated side-chain ionenes, Macromolecules, 30 (24) (1997), pp. 7560-7567
43. S.V. Arehart, C. Pugh, Induction of smectic layering in nematic liquid crystals using immiscible components. 1. Laterally attached side-chain liquid crystalline poly (norbornene) s and their low molar mass analogs with hydrocarbon/fluorocarbon substituents, J. Am. Chem. Soc., 119 (13) (1997), pp. 3027-3037
44. A. Mourran, B. Tartsch, M. Gallyamov, S. Magonov, D. Lambreva, B.I. Ostrovskii, I.P. Dolbnya, W.H. de Jeu, M. Moeller, Self-assembly of the perfluoroalkyl-alkane F14H20 in ultrathin films, Langmuir, 21 (6) (2005), pp. 2308-2316
45. X. Li, L. Andruzzi, E. Chiellini, G. Galli, C.K. Ober, A. Hexemer, E.J. Kramer, D.A. Fischer, Semifluorinated aromatic side-group polystyrene-based block copolymers: bulk structure and surface orientation studies, Macromolecules, 35 (21) (2002), pp. 8078-8087
46. G. Hougham, Fluoropolymers 2: Properties, vol. 2, Springer (1999)
47. N. Terasawa, H. Monobe, K. Kiyohara, Mesomorphic phase transition behavior of novel triphenylene compounds possessing fluoroalkylated side chains, J. Fluorine Chem., 127 (7) (2006), pp. 954-961
48. S. Krishnan, Y.J. Kwark, C.K. Ober, Fluorinated polymers: liquid crystalline properties and applications in lithography, Chem. Rec., 4 (5) (2004), pp. 315-330
49. N. Politakos, C.J. Weinman, M.Y. Paik, H.S. Sundaram, C.K. Ober, A. Avgeropoulos, Synthesis, molecular, and morphological characterization of initial and modified diblock copolymers with organic acid chloride derivatives, J. Polym. Sci., Part A: Polym. Chem., 49 (19) (2011), pp. 4292-4305
50. Fan-Bao Meng, Zhang Xiao-Dong, Xiao-Zhi He, He Lu, Yue Ma, Hui-Li Han, Bao-Yan Zhang, Synthesis and characterization of side-chain liquid crystalline polymers and oriented elastomers containing terminal perfluorocarbon chains, Polymer, 52 (2011), pp. 5075-5508
51. P. Gopalan, L. Andruzzi, X. Li, C.K. Ober, Fluorinated mesogen-jacketed liquid-crystalline polymers as surface-modifying agents: design, synthesis and characterization, Macromol. Chem. Phys., 203 (10–11) (2002), pp. 1573-1583
52. R. Weberskirch, J. Preuschen, H. Spiess, O. Nuyken, Design and synthesis of a two compartment micellar system based on the self-association behavior of poly (N-acylethyleneimine) end-capped with a fluorocarbon and a hydrocarbon chain, Macromol. Chem. Phys., 201 (10) (2000), pp. 995-1007
53. L. Wilson, A. Griffin, Liquid crystalline fluorocarbon side-chain polyesters, Macromolecules, 27 (7) (1994), pp. 1928-1931
54. J. Wang, G. Mao, C.K. Ober, E.J. Kramer, Liquid crystalline, semifluorinated side group block copolymers with stable low energy surfaces: synthesis, liquid crystalline structure, and critical surface tension, Macromolecules, 30 (7) (1997), pp. 1906-1914
55. Y. Ren, T.P. Lodge, M.A. Hillmyer, Effect of selective perfluoroalkylation on the segregation strength of polystyrene-1, 2-polybutadiene block copolymers, Macromolecules, 35 (10) (2002), pp. 3889-3894
56. J. Hao, R.A. Weiss, Mechanical behavior of hybrid hydrogels composed of a physical and a chemical network, Polymer, 54 (8) (2013), pp. 2174-2182

57. J. Hao, R.A. Weiss, Viscoelastic and mechanical behavior of hydrophobically modified hydrogels, Macromolecules, 44 (23) (2011), pp. 9390-9398
58. J. Shen, T. Hogen-Esch, Block copolymer-like self-assembly of fluorocarbon end-functionalized polystyrene and polybutylmethacrylate, J. Am. Chem. Soc., 130 (33) (2008), pp. 10866-10867
59. J. Shen, V.A. Piunova, S. Nutt, T.E. Hogen-Esch, Blends of polystyrene and poly (n-butyl methacrylate) mediated by perfluorocarbon end groups, Polymer, 54 (21) (2013), pp. 5790-5800
60. V.A. Piunova, T.E. Hogen-Esch, Synthesis of telechelic perfluorocarbon functionalized polystyreneand polybutylmethacrylate and characterization of their blends, Polymer, 69 (2015), pp. 58-65
61. J. Shen, Perfluorocarbon Mediated Self-assembly of Polymers, PhD thesis, University of Southern California (August 2009)
62. M. Yurdacan, O. Franke, T.E. Hogen-Esch, Nanoindentation of films of perfluorotridecyl, perfluorodecyl, and perfluoroheptyl end-functionalized polystyrene at the micron scale, Macromol. Chem. Phys., 217 (2016), pp. 1260-1269
63. M. YurdacanInvestigation of Mechanical, Thermal and Rheological Properties of Fluorocarbon Functionalized Polystyrene and Development of Increased Flow Graphene Based Polymer Nanocomposite Membranes, University of Southern California (August 2015)
64. Q. Cao, Y.H. Song, Z.H. Liu, Q. Zheng, Influence of annealing on rheological and conductive behaviors of high-density polyethylene/carbon black composites, J. Mater. Sci., 44 (2009), pp. 4241-4245
65. T. Faravelli, M. Pinciroli, F. Pisano, G. Bozzano, M. Dente, E. Ranzi, Thermal degradation of polystyrene, J. Anal. Appl. Pyrolysis, 60 (2001), pp. 103-121
66. M. Guaita, O. Chiantore, L. Costa, Changes in degree of polymerization in the thermal degradation of polystyrene, Polym. Degrad. Stabil., 12 (1985), pp. 315-332
67. D.A. Anderson, E.S. Freeman, The kinetics of the thermal degradation of polystyrene and polyethylene, J. Polym. Sci., 54 (1961), pp. 253-260
68. G. Madras, G. Chung, J. Smith, B.J. McCoy, Molecular weight effect on the dynamics of polystyrene degradation, Ind. Eng. Chem. Res., 36 (1997), pp. 2019-2024

Please cite the article as: H.M. Yurdacan, X. Li, S. Nutt, T.E. Hogen-Esch, **“Perfluoroalkyl end-functionalized polystyrene show lower glass transition temperatures. DSC and optical transmission studies,”** Polymer 138 (2018) 295-301. DOI: **10.1016/j.polymer.2018.01.061**

Supplementary Materials

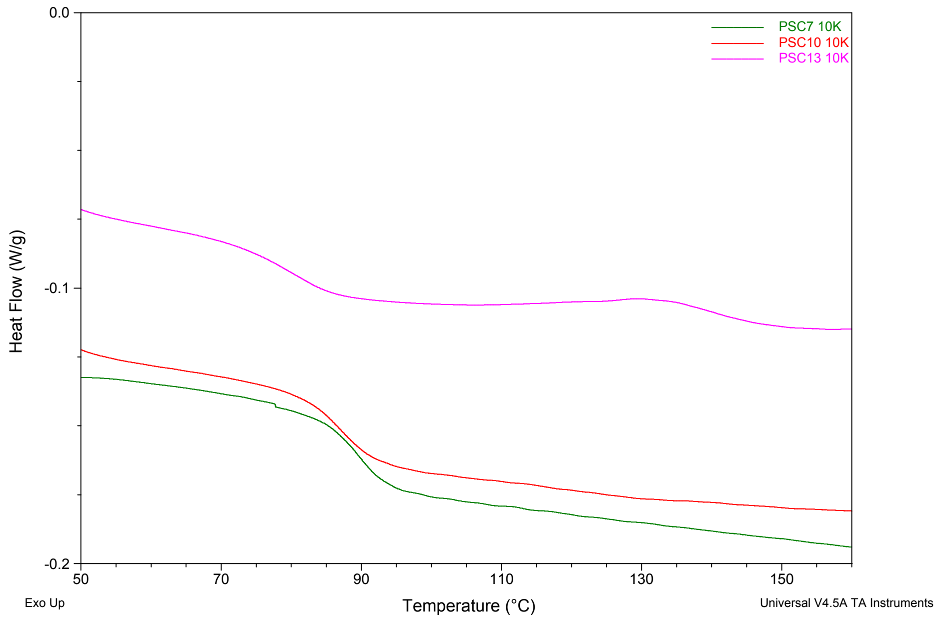

Figure-SI-1. DSC thermograms of PSC7-10K(green), PSC10-10K (red), PSC13-10K (purple). Measurements were taken at second runs and the samples were heated under nitrogen to 180 °C at a rate of 5 °C/min..

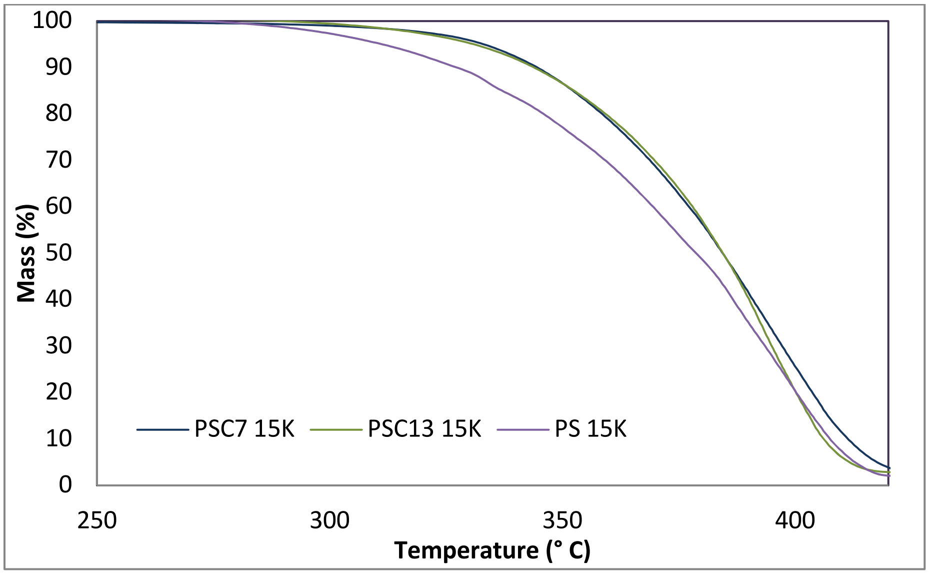

Figure SI-2. TGA curves of PS-15K , PSC7-15K and PSC13-15K.

Please cite the article as: H.M. Yurdacan, X. Li, S. Nutt, T.E. Hogen-Esch, **“Perfluoroalkyl end-functionalized polystyrene show lower glass transition temperatures. DSC and optical transmission studies,”** Polymer 138 (2018) 295-301. DOI: **10.1016/j.polymer.2018.01.061**

Please cite the article as: H.M. Yurdacan, X. Li, S. Nutt, T.E. Hogen-Esch, **"Perfluoroalkyl end-functionalized polystyrene show lower glass transition temperatures. DSC and optical transmission studies,"** Polymer 138 (2018) 295-301. DOI: **10.1016/j.polymer.2018.01.061**